J|A|C|S
ARTICLES
Published on Web 09/09/2006

Controlling the Growth of Single Crystalline Nanoribbons of Copper Tetracyanoquinodimethane for the Fabrication of Devices and Device Arrays

Yaling Liu,[†,‡] Hongxiang Li,[†] Deyu Tu,[‡,§] Zhuoyu Ji,[†,‡] Congshun Wang,[§] Qingxin Tang,[†,‡] Ming Liu,[§] Wenping Hu,*[,†] Yunqi Liu,[†] and Daoben Zhu*[,†]

Contribution from Beijing National Laboratory for Molecular Sciences, Key Laboratory of Organic Solids, Institute of Chemistry, Chinese Academy of Sciences, Beijing 100080, Department of Compound Semiconductor Devices and Circuit, Institute of Microelectronics, Chinese Academy of Sciences, Beijing 100029, and Graduate School of Chinese Academy of Sciences, Beijing 100039, P. R. China

Received May 31, 2006; E-mail: huwp@iccas.ac.cn; zhudb@iccas.ac.cn

Abstract: In this paper, (1) a simple and controllable method to synthesize single crystalline nanoribbons of CuTCNQ in a large area was demonstrated by using a physical and chemical vapor combined deposition technique. (2) Nanoribbons synthesized by this method were identified to belong to phase I. (3) Devices and device arrays of nanoribbons were in situ fabricated by this method using gap electrodes and gap electrode arrays. (4) Current−voltage characteristics of crystalline devices and device arrays of nanoribbons exhibited semiconductor properties, and this conclusion was further confirmed by the results of devices based on an individual nanoribbon or microribbon of CuTCNQ (phase I). The controllable synthesis of nanoribbons for the in situ fabrication of crystalline nanodevices and device arrays will be attractive for nanoelectronics. Moreover, semiconductor current−voltage characteristics of the nanoribbons will be beneficial to the understanding of CuTCNQ.

Introduction

Nanowires/nanoribbons can act as both active devices and interconnects and have been regarded as a "bottom-up" paradigm of nanoelectronics.[1] For example, individual semiconducting nanowire has been configured as field-effect transistor,[1b] photodetector,[1c] and bio/chemical sensor.[1d] Crossed nanowire/nanoribbon architecture enables diverse functions simply through choice of nanowire/nanoribbon building blocks and provides possibilities for scalable integration to the highest densities.[1e−h] Hence, the synthesis of nanowires/nanoribbons with functions has attracted particular attention recently.[1] It is especially true for single crystalline nanowires/nanoribbons because single crystals indeed reveal intrinsic properties of materials and open up prospects for high-quality devices and circuits.

Copper tetracyanoquinodimethane (CuTCNQ), which is believed to be an organic switching and memory material, has drawn interest since the 1970s (for the molecular structure of TCNQ and the synthesis of CuTCNQ see the Supporting Information).[2] Despite extensive effort devoted to understanding the electrical switching of CuTCNQ, there remains skepticism regarding the switching of the material. It has been suggested by some researchers that the electrical switching behavior is related not to changes in the bulk sample but to the formation of channels created from the contact of the aluminum electrode with the irregular surface of the CuTCNQ films.[3] The arising skepticism is probably because (1) most reported devices adopted a sandwich structure (e.g., Cu/CuTCNQ/Al) which was fabricated on polycrystalline films generated by "spontaneous electrolysis". The polycrystalline film was always loosely packed so that metal atoms easily diffused into the film in the process

† Beijing National Laboratory for Molecular Sciences, Chinese Academy of Sciences.
‡ Graduate School of Chinese Academy of Sciences.
§ Department of Compound Semiconductor Devices and Circuit, Chinese Academy of Sciences.

(1) (a) Wu, Y.; Xiang, J.; Yang, C.; Lu, W.; Lieber, C. M. *Nature* **2004**, *430*, 61−65. (b) Tans, S. J.; Verschueren, A. R. M.; Dekker, C. *Nature* **1998**, *393*, 49−52. (c) Wang, J. F.; Gudiksen, M. S.; Duan, X. F.; Cui, Y.; Lieber, C. M. *Science* **2001**, *293*, 1455−1457. (d) Klemic, J. F.; Stern, E.; Reed, M. A. *Nat. Biotechnol.* **2001**, *19*, 924−925. (e) Thurn-Albrecht, T.; Schotter, J.; Kästle, G. A.; Emley, N.; Shibauchi, T.; Krusin-Elbaum, L.; Guarini, K.; Black, C. T.; Tuominen, M. T.; Russell, T. P. *Science* **2000**, *290*, 2126−2129. (f) Beckman, R.; Johnston-Halperin, E.; Luo, Y.; Green, J. E.; Heath, J. R. *Science* **2005**, *310*, 465−468. (g) Melosh, N. A.; Boukai, A.; Diana, F.; Gerardot, B.; Badolato, A.; Petroff, P. M.; Heath, J. R. *Science* **2003**, *300*, 112−115. (h) Wang, X.; Zhuang, J.; Peng, Q.; Li, Y. D. *Nature* **2005**, *437*, 121−124.

(2) (a) Potember, R. S.; Poehler, T. O.; Cowan, D. O. *Appl. Phys. Lett.* **1979**, *34*, 405−407. (b) Potember, R. S.; Poehler, T. O.; Rappa, A.; Cowan, D. O.; Bloch, A. N. *J. Am. Chem. Soc.* **1980**, *102*, 3659−3660. (c) Potember, R. S.; Poehler, T. O.; Benson, R. C. *Appl. Phys. Lett.* **1982**, *41*, 548−550. (d) Neufeld, A. K.; Madsen, I.; Bond, A. M.; Hogan, C. F. *Chem. Mater.* **2003**, *15*, 3573−3585. (e) Kamitsos, E. I.; Risen, W. M. *J. Chem. Phys.* **1983**, *79*, 5808−5819. (f) Hu, Z. P.; Shen, Z. X.; Qin, L.; Tang, S. H.; Kuok, M. H.; Xu, G. Q.; Mok, K. F.; Huang, H. H. *J. Mol. Struct.* **1995**, *356*, 163−168. (g) Harris, M.; Hoagland, J. J.; Mazur, U.; Hipps, K. W. *Vib. Spectrosc.* **1995**, *9*, 273−277. (h) Potember, R. S.; Poehler, T. O.; Cowan, D. O.; Carter, F. L.; Brant, P. I. In *Molecular Electronic Devices*; Carter, F. L., Ed.; Marcel Dekker: New York, 1982; p 73. (i) Harris, A. R.; Neufeld, A. K.; O'Mullane, A. P.; Bond, A. M.; Morrison, R. J. S. *J. Electrochem. Soc.* **2005**, *152*, C577−C583. (j) Neufeld, A. K.; O'Mullane, A. P.; Bond, A. M. *J. Am. Chem. Soc.* **2005**, *127*, 13846−13853. (k) O'Mullane, A. P.; Neufeld, A. K.; Bond, A. M. *Anal. Chem.* **2005**, *77*, 5447−5452.

(3) (a) Duan, H.; Mays, M. D.; Cowan, D. O.; Kruger, J. *Synth. Met.* **1989**, *28*, 675−680. (b) Sato, C.; Wakamatsu, S.; Tadokoro, K.; Ishii, K. *J. Appl. Phys.* **1990**, *68*, 6535−6537. (c) Hoagland, J. J.; Wang, X. D.; Hipps, K. W. *Chem. Mater.* **1993**, *5*, 54−60.

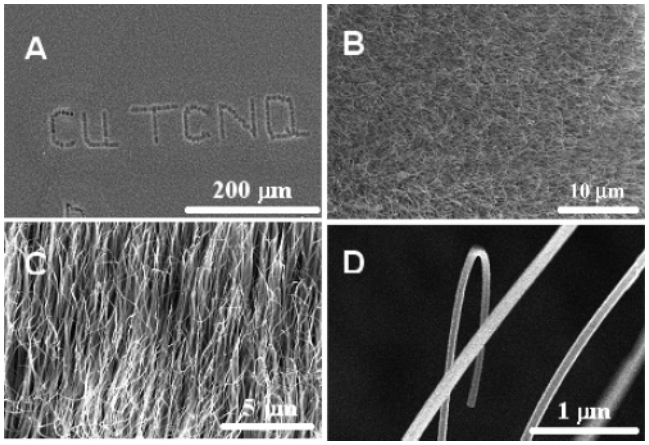

Figure 1. (A, B) Top view of CuTCNQ nanoribbon layer prepared in a large area. (C) Nanoribbon arrays synthesized in the low-temperature region (70 °C) with Ar gas flow rate of 150 sccm through a rectangular tube passing the Cu surface and a 2 h reaction time. (D) Enlarged SEM image of several nanoribbons.

of electrode deposition, leading to doping or even leakage of the device. Therefore, the reproducibility of CuTCNQ devices was rather low and the thickness of the CuTCNQ film was required to be very thick.[2] (2) As we know, aluminum easily causes Schottky contact with organic materials; hence, the top contact between CuTCNQ and Al in Cu/CuTCNQ/Al sandwich devices was also questionable.[3] (3) Dunbar et al. demonstrated that there are two distinct polymorphs of CuTCNQ: the "needle or rodlike" kinetic product of phase I and the "platelet-like" thermodynamically stable material of phase II.[4] These two phases both can be synthesized via "spontaneous electrolysis". The kinetic product (phase I) is soluble in acetonitrile and slowly converts to a more thermodynamically stable material (phase II). Both phases are dark purple, crystalline materials. Their chemical composition and electronic characteristics are identical, but the structures and properties are quite different. (e.g., the conductivity of phase I was found to be high but that of phase II was rather low).[4] Both phases easily present in thin films of CuTCNQ grown on copper substrates simultaneously, and any subtle difference in reaction conditions can lead to variable quantities of the two phases. Undoubtedly, this is an important cause of the reported inconsistencies in the properties of CuTCNQ devices.[4]

We have been concentrating on CuTCNQ for some years[5] and acknowledged the problems encountered with its devices. We believe that it is imperative to clarify the phase dependence of the intrinsic properties of CuTCNQ for its practical application, i.e., which phase is probably responsible for the switching effect. For this aim, the problems that needed to be explored are (a) how to get CuTCNQ products with pure phase I or phase II, instead of the usual mixture of both phases by "spontaneous electrolysis"; (b) how to solve the problems encountered with sandwich devices, such as the leakage caused by the diffusion

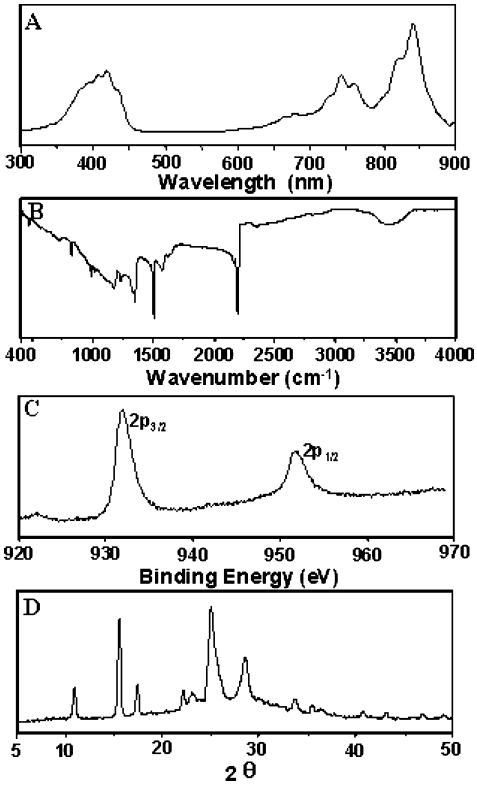

Figure 2. (A) UV−vis, (B) FTIR, (C) XPS, and (D) XRD pattern of CuTCNQ nanoribbons. The UV−vis was recorded at room temperature by dissolving CuTCNQ nanoribbons in acetonitrile, FTIR was performed by using pressed pellets of a mixture of the nanoribbons and KBr (the peak at 3400 cm^{-1} was due to the adsorbed water of KBr), and XPS and XRD were measured using CuTCNQ nanoribbons layer.

of the top electrode during the vacuum deposition and the top contact effect between the CuTCNQ and the Al electrode; and (c) how to examine the intrinsic properties of CuTCNQ. Actually, these problems are the focus of our present paper.

A method that combined physical and chemical vapor deposition techniques was developed to synthesize phase I single crystalline nanoribbons of CuTCNQ in a large area. And such nanoribbons could also be in situ synthesized between Au gap electrodes for the fabrication of crystalline devices and device arrays, so that we can not only circumvent the inherent problems of sandwiched devices encountered but also reveal the intrinsic properties of CuTCNQ. Moreover, the combination of CuTCNQ with nanodevices, i.e., the use of CuTCNQ nanoribbons for the fabrication of nanodevices and devices arrays, is definitely attractive for nanoelectronics, too.[1]

Results and Discussion

Recently, Liu et al. reported that CuTCNQ nanowires could be prepared by an organic solid-phase reaction,[5f] i.e., TCNQ powder was loaded in a ceramic boat, covered with copper foil, and heated at 120 °C for 2 h. They have applied the film of the nanowires in field emitters successfully, although the structure (crystalline or amorphous) and phase (phase I or phase II) of such nanowires were unclear at that time. We reproduced the synthesis of CuTCNQ nanowires by their method to try to extend the nanowires into devices, but found the controllability of their method for devices fabrication was challenging, i.e., it was difficult to separate an individual nanowire for devices fabrication. However, evoked by their method and our recent

(4) Heintz, R. A.; Zhao, H.; Ouyang, X.; Grandinetti, G.; Cowen, J.; Dunbar, K. R. *Inorg. Chem.* **1999**, *38*, 144−156.
(5) (a) Liu, S. G.; Liu, Y. Q.; Wu, P. J.; Zhu, D. B. *Chem. Mater.* **1996**, *8*, 2779−2787. (b) Liu, S. G.; Liu, Y. Q.; Zhu, D. B. *Thin Solid Films* **1996**, *280*, 271−277. (c) Sun, S. Q.; Wu, P. J.; Zhu, D. B. *Solid State Commun.* **1996**, *99*, 237−240. (d) Liu, S. G.; Liu, Y. Q.; Wu, P. J.; Zhu, D. B.; Tian, H.; Chen, K. C. *Thin Solid Films* **1996**, *289*, 300−305. (e) Liu, Y.; Ji, Z.; Tang, Q.; Jiang, L.; Li, H.; He, M.; Hu, W.; Zhang, D.; Jiang, L.; Wang, X.; Wang, C.; Liu, Y.; Zhu, D. *Adv. Mater.* **2005**, *17*, 2953−2957. (f) Liu, H.; Zhao, Q.; Li, Y.; Liu, Y.; Lu, F.; Zhuang, J.; Wang, S.; Jiang, L.; Zhu, D.; Yu, D.; Chi, L. *J. Am. Chem. Soc.* **2005**, *127*, 1120−1121.

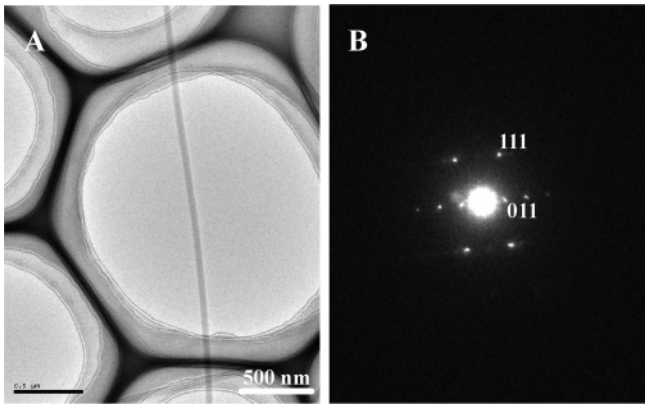

Figure 3. (A) A TEM micrograph of an individual nanoribbon and (B) its corresponding electron diffraction pattern.

method for the synthesis of nanoribbons of copper phthalocyanine[7a] (physical vapor transport technique), we developed a new method to synthesize single crystalline nanoribbons of CuTCNQ in a large area.

A two-zone physical vapor deposition (PVD) system was used in the experiment (for details see the Supporting Information). TCNQ powder was placed at the high-temperature zone and vaporized at ~220 °C. Cu plates (or Cu covered Si/glass substrates) were placed at the low-temperature zone. TCNQ vapor was carried by flowing Ar and reacted with Cu at the low-temperature zone. Dark blue fuzzlike products, which were found to be CuTCNQ nanoribbons later, were obtained on the substrates. The growth process of nanoribbons here is similar to that in a low vacuum chemical vapor deposition (CVD) system. TCNQ vapor (precursor) approaches the Cu surface and reacts with Cu to form nanoribbons. Hence we call this method a PVD and CVD combined technique.

CuTCNQ nanoribbons were synthesized in a large area by this method, as shown in Figure 1A,B. The growth mechanism of nanoribbons was noted, although it has not been fully understood yet. The initial products observed on Cu substrate were CuTCNQ dots. These dots gradually grew into nanorods and finally evolved into long nanoribbons (see the Supporting Information). The growth process of the nanoribbons could be adjusted by several experimental conditions, such as reaction temperature, reaction time, and Ar flow rate, similar to the typical physical vapor transport technique[7] (see the Supporting Information). For example, CuTCNQ nanoribbon arrays could be obtained by adjusting Ar flow rate and direction (Figure 1C). An enlarged SEM image of several nanoribbons of Figure 1C is shown in Figure 1D. It was found that the length of the nanoribbons could range from several to several tens of micrometers, and the width of the nanoribbons ranged from several tens to several hundreds of nanometers (see the Supporting Information).

Similar to the nanorods that we reported previously,[5e] nanoribbons obtained in this study also belong to phase I,[4] as evidenced by the characterizations presented in Figure 2. The absorption spectrum of the nanoribbons was shown in Figure

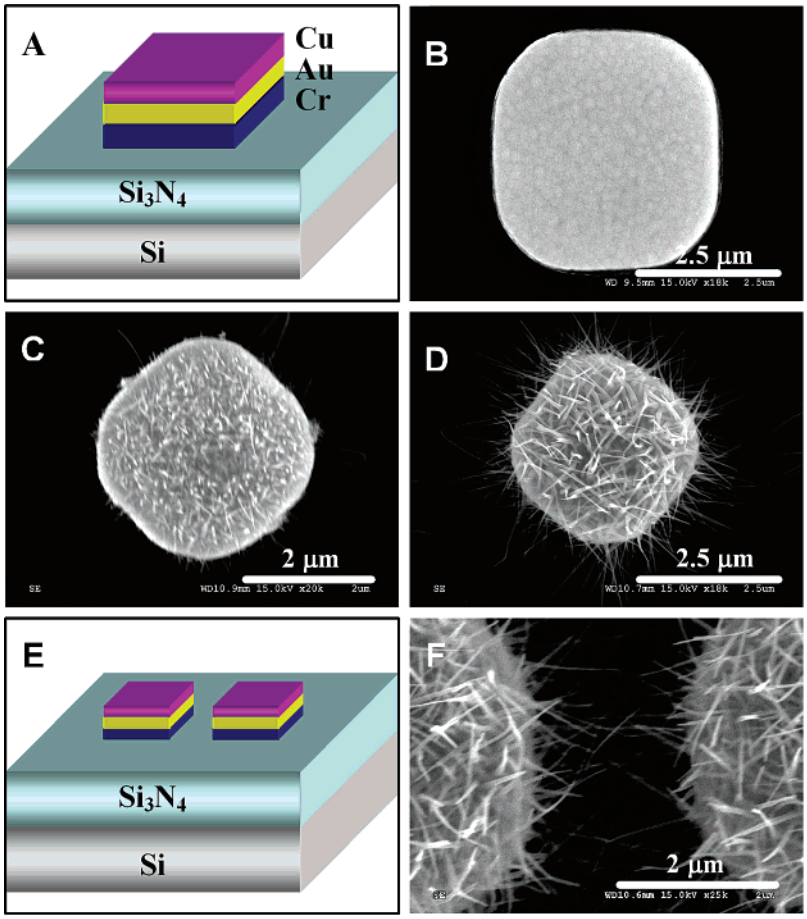

Figure 4. (A, E) Schematic view of Cr/Au/Cu multilayer pads prepared by photolithography on Si/Si_3N_4 substrate, (B) SEM image of a pad, (C, D) CuTCNQ nanoribbons grown gradually, and (F) CuTCNQ nanoribbons striding over the gap of two pads to connect them together.

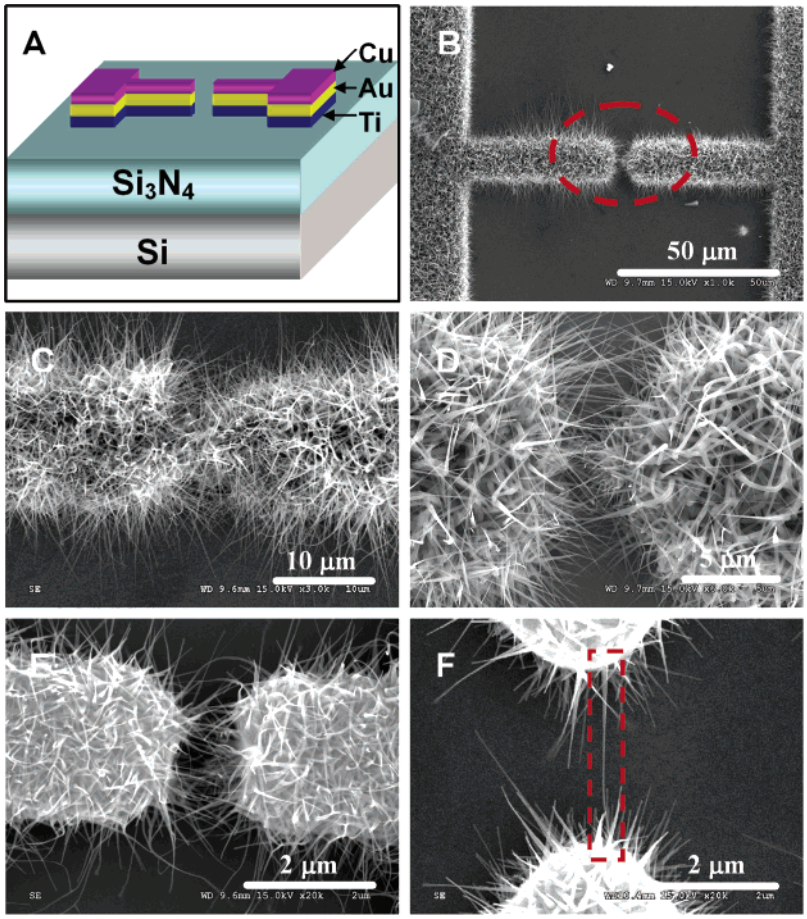

Figure 5. (A) Schematic view of Ti/Au/Cu multilayer gap electrodes. (B) Gap electrodes connected by CuTCNQ nanoribbons. Through changing the temperature of the gap electrodes, the number of connected nanoribbons between the gap electrodes could be adjusted, with reaction time 120 min and Ar gas flow rate 225 sccm: (C) at ~200 °C there was a large amount of connected nanoribbons, (D) at ~150 °C, there was several tens of connected nanoribbons, (E) at ~120 °C, there was about 10 connected nanoribbons, (F) at ~70 °C, the device is based on an individual nanoribbon of CuTCNQ.

2A, and the peaks at ~420, 742, and 841 nm were assigned to the TCNQ anion radical of CuTCNQ.[5,8] Figure 2B showed FTIR spectrum of the nanoribbons. The band at 2200 cm^{-1} was the typical absorption of C≡N stretching, and the weak absorption at 1577 and 1506 cm^{-1} was assigned to C═C ring stretching. The C═C ring stretching region was also characterized by the band at around 1351 cm^{-1}. The peak at ~3400 cm^{-1} in the FTIR was not assigned to the nanoribbons but to water adsorbed by KBr substrates during the measuring process. XPS data of the nanoribbons gave the $Cu2p_{3/2}$ and $Cu2p_{1/2}$ signals depicted in Figure 2C, which exhibited no evidence for shoulders or satellites due to Cu(II), suggesting that the products were essentially Cu(I). Meanwhile, the N1s orbitals appeared as a single feature at 398.8 eV, which was indicative of one type of TCNQ.[2h,4] The XRD powder pattern of the nanoribbons was given in Figure 2D, which showed a few intense features in the low-angle region. These features identified that nanoribbons belonged to phase I with a tetragonal cell.[4] The selected-area electron diffraction (SAED) pattern of the nanoribbons further confirmed this conclusion; i.e., the nanoribbons belong to phase I. Given in Figure 3A was a typical TEM image of the nanoribbons, and the corresponding SAED pattern was shown in Figure 3B. No change of the SAED pattern was observed for the different part of the same nanoribbon, indicating that the whole nanoribbon was a single crystal. It could be determined from the SAED pattern that the nanoribbons had

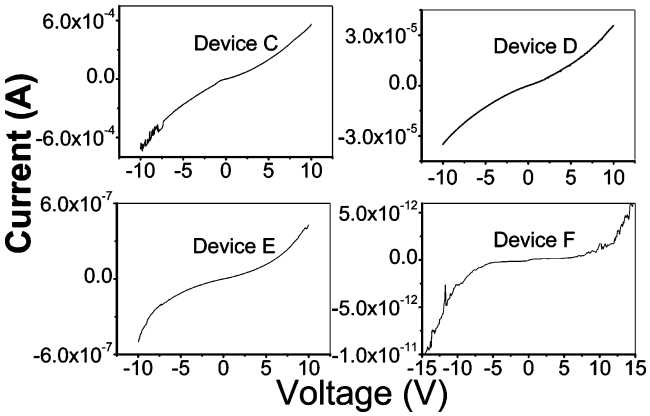

Figure 6. The corresponding *I*−*V* characteristics of devices shown in Figure 5C−F.

the unit cell of phase I CuTCNQ, as reported in ref 4. The extinction of 100 agreed with space group *Pn* assigned by Dunbar et al.[4] It could be also revealed from Figure 3B that the nanoribbons grew along the [100] direction, coinciding with the fact that CuTCNQ molecules stacked up along this direction through strong $\pi-\pi$ interaction.

A Cr/Au/Cu multilayer pad prepared by photolithography on Si/Si_3N_4 substrate (Figure 4A,B) was inserted into our system for nanoribbons growth. As soon as the pad contacted with TCNQ vapor, Cu on the pad surface reacted with TCNQ im-

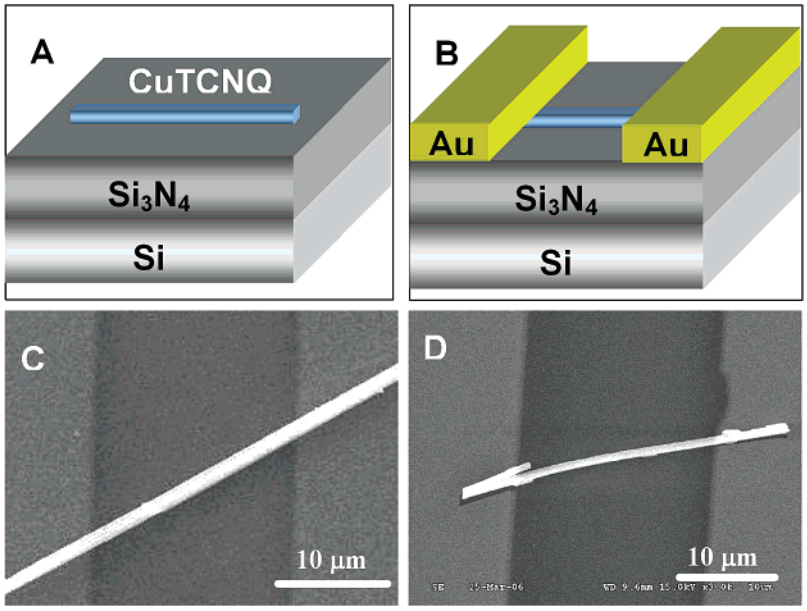

Figure 7. (A, B) Schematic view of device fabrication based on an individual submicrometer-sized ribbon of CuTCNQ and (C, D) SEM images of a device based on an individual submicrometer-sized ribbon of CuTCNQ which was fabricated using the method described in ref 7a.

mediately and CuTCNQ (Figure 4C) was grown. With the reaction continuing, CuTCNQ nanoribbons grew gradually (Figure 4D) and tended to stride over the gap between the two pads and connect them together (Figure 4E,F). Hence, this is a prospective method to fabricate CuTCNQ single crystalline devices.

Encouraged by this finding, Ti/Au/Cu multilayer gap electrodes were prepared by photolithography on Si/Si_3N_4 substrate (Figure 5A) with a gap width of several micrometers (the last layer, the Cu layer could also be prepared by an electroplating technique on Ti/Au gap electrodes). The top Cu layer could react with TCNQ vapor to generate CuTCNQ nanoribbons, and then nanoribbons would stretch toward each other and finally connect the gap electrodes together (Figure 5B). The number of connected nanoribbons between gap electrodes could be adjusted by changing the experimental conditions (see Figure 5C−F and the Supporting Information).

Typical current−voltage ($I-V$) characteristics showed that the above devices behaved as semiconductors (Figure 6). The symmetrical $I-V$ characteristics of devices illustrated in Figure 5C−E suggested possible symmetrical connections at both ends of the nanoribbons or an average effect of a large amount of asymmetrical connection of the nanoribbons. The asymmetrical $I-V$ characteristics of the device shown in Figure 5F indicated asymmetrical ends connecting the single nanoribbon. The device current of an individual nanoribbon was much smaller than that of the others, which was not only due to the decrease of connected nanoribbons between gap electrodes but also to the width difference at both ends of the nanoribbon. Anyway, the

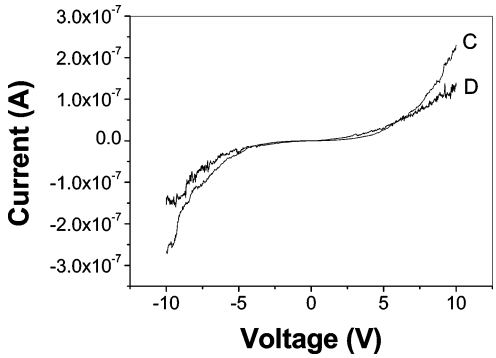

Figure 8. $I-V$ characteristics of devices illustrated in Figure 7.

semiconductor behaviors of all devices agreed well, which indicated that the material responsible for switching was not our nanoribbons (phase I).

In order to further confirm this, higher voltage was applied to the devices shown in Figure 5 until they were broken. No switching phenomenon was observed in all devices. Moreover, devices based on an individual crystal at submicrometer (Figure 7) level were fabricated by the "multi times gold wire mask moving" technique.[7] Submicrometer-sized ribbons of CuTCNQ were obtained in our PVD system by adjusting the reaction time, which gave an identical crystal stack as that of our nanoribbons. The $I-V$ characteristics of devices based on micrometer-sized ribbons were similar to those shown in Figure 6; i.e., these devices behaved as semiconductors and no switching phenomenon was observed. Results were illustrated in the plot of Figure 8. Dunbar et al.[4] once suggested that the material responsible for switching in CuTCNQ films was not phase I. Our results of nano- and microribbons highly accorded with their conclusion.

Finally, it should be mentioned that device arrays of CuTCNQ nanoribbons could be fabricated by the same principle by using arrays of Cr/Au/Cu multilayer pads (Figure 9). The $I-V$ characteristics of such devices further confirmed our conclusion that CuTCNQ nanoribbons behaved as semiconductors. Certainly, it should be emphasized here that this conclusion does not mean CuTCNQ is not a switching material; the results here

(6) (a) De Boer, R. W. I.; Klapwijk, T. M.; Morpurgo, A. F. *Appl. Phys. Lett.* **2003**, *83*, 4345−4347. (b) Takeya, J.; Goldmann, C.; Hass, S.; Pernstich, K. P.; Ketterer, B.; Batlogg, B. *J. Appl. Phys.* **2003**, *94*, 5800−5804. (c) Mas-Torrent, M.; Durkut, M.; Hadley, P.; Ribas, X.; Rovira, C. *J. Am. Chem. Soc.* **2004**, *126*, 984−985. (d) Moon, H.; Zeis, R.; Borkent, E.-J.; Besnard, C.; Lovinger, A. J.; Siegrist, T.; Kloc, C.; Bao, Z. *J. Am. Chem. Soc.* **2004**, *126*, 15322−15323.
(7) (a) Tang, Q.; Li, H.; He, M.; Hu, W.; Liu, C.; Chen, K.; Wang, C.; Liu, Y.; Zhu, D. *Adv. Mater.* **2006**, *18*, 65−68. (b) Laudise, R. A.; Kloc, Ch.; Simpkins, P. G.; Siegrist, T. *J. Cryst. Growth* **1998**, *187*, 449−454.
(8) (a) Melby, L. R.; Harder, R. J.; Hertler, W. R.; Mahler, W.; Benson, R. E.; Mochel, W. E. *J. Am. Chem. Soc.* **1962**, *84*, 3374−3387. (b) Jeanmaire, D. L.; Van Duyne, R. P. *J. Am. Chem. Soc.* **1976**, *98*, 4029−4033. (c) Gong, J. P.; Osada, Y. *Appl. Phys. Lett.* **1992**, *61*, 2787−2789.

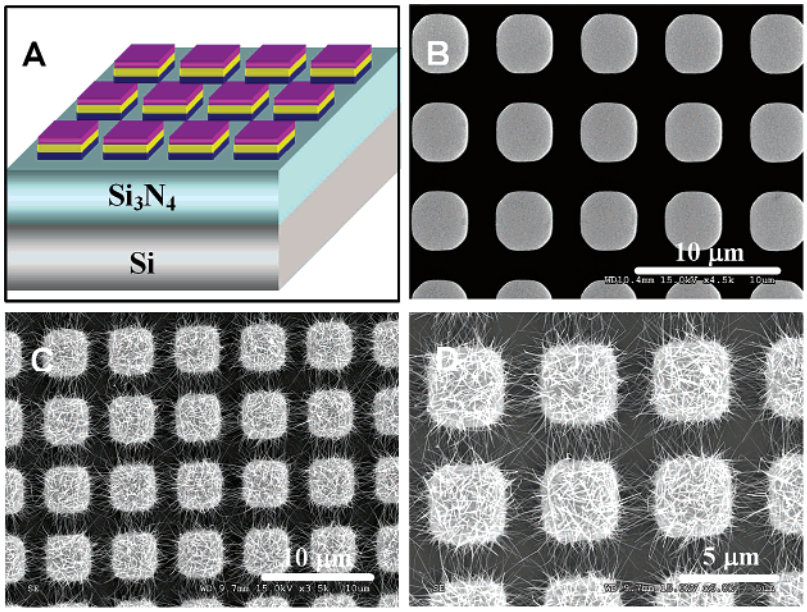

Figure 9. (A) Schematic arrays of Cr/Au/Cu multilayer pads, (B) SEM image of pad arrays, and (C, D) device arrays of CuTCNQ nanoribbons.

only indicate that the material responsible for switching is not our nanoribbons (phase I). Factually, we have observed highly reproducible switching in devices of CuTCNQ in other phase status (the detailed mechanism is still under examination).

Conclusions

In summary, in this paper, we demonstrated a simple and controllable method to in situ synthesize single crystalline nanoribbons of CuTCNQ by using a combined physical and chemical vapor deposition technique. Nanoribbons synthesized by this method were identified as belonging to phase I. Crystalline devices and device arrays of nanoribbons were in situ fabricated by this method using gap electrodes and gap electrode arrays. Current−voltage characteristics of crystalline devices and device arrays of nanoribbons exhibited semiconductor properties, and this conclusion was further confirmed by the results of devices based on an individual nanoribbon or microribbon of CuTCNQ (phase I). The controllable synthesis of nanoribbons and the in situ fabrication of crystalline devices and device arrays based on nanoribbons will be attractive for nanoelectronics. Semiconductor current−voltage characteristics of nanoribbons will be beneficial for the understanding of CuTCNQ.

Experimental Section

Products were characterized by UV−vis (U3010), Fourier-transform infrared spectroscopy (FTIR, PE2000), X-ray photoelectron spectroscopy (XPS, ESCALab220I-XL), X-ray diffraction (XRD, D/max2500), scanning electron microscopy (SEM, Hitachi S-4300 SE), and transmission electron microscopy (TEM, JEOL 2010).

Ti/Au/Cu (or Cr/Au/Cu) multilayer pad, pad arrays, and gap electrodes were prepared by photolithography. Nanoribbons of CuTCNQ were in situ synthesized on the pads or between the gap electrodes. A Keithley 4200 SCS was used for the current−voltage characterization of the nanoribbons.

Acknowledgment. W.H. is grateful to Prof. Chen Wang (National Center for Nanoscience and Technology) and Dr. Meng He (National Center for Nanoscience and Technology) for discussions. The authors acknowledge financial support from National Natural Science Foundation of China (20421101, 20404013, 20402015, 20571079, 20527001, 90401026, 20472089, 90206049), Ministry of Science and Technology of China and Chinese Academy of Science. This paper is dedicated for the 50th anniversary of Institute of Chemistry, Chinese Academy of Science.

Supporting Information Available: The molecular structure of TCNQ; the schematic reaction of TCNQ and Cu; the preparation of single crystalline CuTCNQ nanoribbons; the possible growth process of nanoribbons; the influence of experimental conditions such as the thickness of Cu film, reaction temperature, reaction time and Ar flow rate; the length and width of nanoribbons; and the adjustment of connection nanoribbons between gap electrodes. This material is available free of charge via the Internet at http://pubs.acs.org.

JA0636183